

Platinum(II)-Mediated Coupling Reactions of Acetonitrile with the Exocyclic Nitrogen of 9-Methyladenine and 1-Methylcytosine. Synthesis, NMR Characterization, and X-ray Structures of New Azametallacycle Complexes

Bruno Longato,^{*,†,‡} Diego Montagner,[‡] Giuliano Bandoli,[§] and Ennio Zangrando[⊥]

Istituto di Scienze e Tecnologie Molecolari-C.N.R., c/o Dipartimento di Scienze Chimiche, Università di Padova, Via Marzolo 1, 35131-Padova, Italy, Dipartimento di Scienze Farmaceutiche, Università di Padova, Via Marzolo 5, 35131-Padova, Italy, and Dipartimento di Scienze Chimiche, Università di Trieste, Via Giorgieri 1, 34127 Trieste, Italy

Received October 10, 2005

The hydroxo complex $cis\text{-}[L_2Pt(\mu\text{-OH})_2](NO_3)_2$ ($L = P\text{MePh}_2$, **1a**), in CH_3CN solution, deprotonates the NH_2 group of 9-methyladenine (9-MeAd) to give the cyclic trinuclear species $cis\text{-}[L_2Pt\{9\text{-MeAd}(-H)\}]_3(NO_3)_3$ ($L = P\text{MePh}_2$, **2a**), in which the nucleobase binds the metal centers through the N(1), N(6) atoms. In solution at room temperature, **2a** slowly reacts with the solvent to form quantitatively the mononuclear azametallacycle $cis\text{-}[L_2PtNH=C(\text{Me})\{9\text{-MeAd}(-2H)\}]NO_3$ ($L = P\text{MePh}_2$, **3a**), containing as anionic ligand the deprotonated form of molecule *N*-(9-methyl-1,9-dihydro-purin-6-ylidene)-acetamidine. In the same experimental conditions, the hydroxo complex with PPh_3 (**1b**) forms immediately the insertion product **3b**. Single-crystal X-ray analyses of **3a** and **3b** show the coordination of the platinum cation at the N(1) site of the purine moiety and to the N atom of the inserted acetonitrile, whereas the exocyclic amino nitrogen binds the carbon atom of the same CN group. The resulting six-membered ring is slightly distorted from planarity, with carbon–nitrogen bond distances for the inserted nitrile typical of a double bond [$C(3)\text{--}N(2) = 1.292(7)$ Å in **3a** and $1.279(11)$ Å in **3b**], while the remaining CN bonds of the metalocycle are in the range of $1.335(8)\text{--}1.397(10)$ Å. A detailed multinuclear 1H , ^{31}P , ^{13}C , and ^{15}N NMR study shows that the nitrogen atom of the inserted acetonitrile molecule binds a proton suggesting for **3a,b** an imino structure in solution. In DMSO and chlorinated solvents, **3a** slowly releases the nitrile reforming the trinuclear species **2a**, whereas **3b** forms the mononuclear derivative $cis\text{-}[L_2Pt\{9\text{-MeAd}(-H)\}]NO_3$ ($L = PPh_3$, **4b**), in which the adeninate ion chelates the metal center through the N(6) and N(7) atoms. Complex **4b** is quantitatively obtained when **1b** reacts with 9-MeAd in DMSO and can be easily isolated if the reaction is carried out in CH_2Cl_2 . In CH_3CN solution, at room temperature, **4b** slowly converts into **3b** indicating that the insertion of acetonitrile is a reversible process. A similar metal-mediated coupling reaction occurs when **1a,b** react with 1-methylcytosine (1-MeCy) in CH_3CN . The resulting complexes, $cis\text{-}[L_2PtNH=C(\text{Me})\{1\text{-MeCy}(-2H)\}]NO_3$ ($L = P\text{MePh}_2$, **5a** and PPh_3 , **5b**), contain the deprotonated form of the ligand *N*-(1-methyl-2-oxo-2,3-dihydro-1*H*-pyrimidin-4-ylidene)-acetamidine. The X-ray analysis of **5a** shows the coordination of the metal at the N(3) site of the pyrimidine cycle and to the nitrogen atom of the acetonitrile, with features of the six-membered metalocycle only slightly different from those found in **3a** and **3b**. In $CD_3CN/CH_3^{13}CN$ solution complexes **5a,b** undergo exchange of the inserted nitrile, while in DMSO or chlorinated solvents they *irreversibly* release CH_3CN to form species not yet fully characterized. No insertion of CH_3CN occurs when the hydroxo complexes are stabilized by PMe_3 and PMe_2Ph .

Introduction

The chemistry of metal-activated organonitriles (RCN) is still intensively investigated owing to the wide variety of products obtainable by addition reactions to the $C\equiv N$

functionality.¹ It is now clear that the coordination of $RC\equiv N$ to a metal center [M] increases the rate of the nucleophilic attack to the carbon atom of the CN group. Depending on the nature of the nucleophile (Nu)—protic or aprotic—the product is the imino derivative, $[M]\text{-NH}=\text{C}(\text{Nu})R$, or the

* To whom correspondence should be addressed. E-mail: longato@chin.unipd.it.

[†] Istituto di Scienze e Tecnologie Molecolari, Università di Padova.

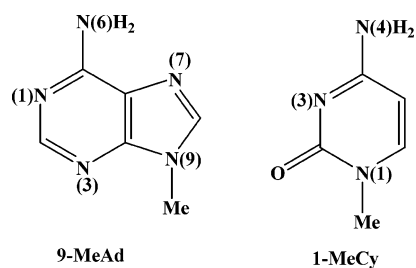
[‡] Dipartimento di Scienze Chimiche, Università di Padova.

[§] Dipartimento di Scienze Farmaceutiche, Università di Padova.

[⊥] Università di Trieste.

(1) (a) Kukushkin, V. Yu.; Pombeiro, A. J. L. *Chem. Rev.* **2002**, *102*, 1771–1802. (b) Michelin, R. A.; Mozzon, M.; Bertani, R. *Coord. Chem. Rev.* **1996**, *147*, 299–338. (c) Reisner, E.; Arion, V. B.; Chioresku, J.; Schmid, W. F. *J. Chem. Soc., Dalton Trans.* **2005**, 2355–2364.

Chart 1



azavinyledene species $[M]-N=C(Nu)R$, respectively. As an example of the first type of reaction, we have recently reported the characterization of the amidine complex $cis-[(PMe_3)_2Pt\{NH=C(Me)NH_2\}\{1-MeTy(-H)\}]^+$ in which 1-MeTy(-H) is the anion of the model nucleobase 1-methylthymine, metal coordinated at the N(3) site. The compound was obtained in low yield from the cationic species $cis-[(PMe_3)_2Pt(N\equiv CMe)\{1-MeTy(-H)\}]^+$, left in acetonitrile containing stoichiometric amounts of water.²

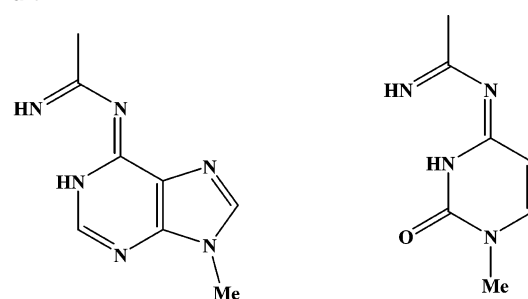
Azavinyledene complexes can be obtained by formal addition of a metal–ligand fragment to a nitrile triple bond. Insertion of acetonitrile into metal–nitrogen bonds of early transition metal amides, $M-NR_2$, to form the adducts $[M]-N=C(Me)NR_2$ is well documented ($M = Ta^3$), and a similar reaction occurs with $M-PR_2$ bonds ($M = Zr$), generating phosphorus analogues of *N,N*-dialkylamidinates.⁴

In this Article we report four examples of insertion of acetonitrile into platinum–nitrogen bonds of the NH_2 -deprotonated nucleobases 9-methyladenine (9-MeAd) and 1-methylcytosine (1-MeCy), depicted in Chart 1, observed in the reactions of the hydroxo complexes $cis-[L_2Pt(\mu-OH)]_2(NO_3)_2$ ($L = PPh_2, PPh_3$) with the model nucleobases in CH_3CN solution.

The structures of the new complexes have been elucidated by single-crystal X-ray analysis and multinuclear NMR spectroscopy showing that in solution they can be formulated as mononuclear azametallacycle species, $cis-[L_2PtNH=C(Me)\{9-MeAd(-2H)\}]^+$ and $cis-[L_2PtNH=C(Me)\{1-MeCy(-2H)\}]^+$ ($L = PPh_2, PPh_3$), in which the anionic ligands are the deprotonated forms of the amidines *N*-(9-methyl-1,9-dihydro-purin-6-ylidene)-acetamide and *N*-(1-methyl-2-oxo-2,3-dihydro-1*H*-pyrimidin-4-ylidene)-acetamide, respectively, shown in Chart 2.

The stability in solution of this new class of metalocycles has been also investigated showing that $cis-[L_2PtNH=C(Me)\{9-MeAd(-2H)\}]^+$ in chlorinated solvents release reversibly the inserted CH_3CN molecule to form the cyclic species $cis-[L_2Pt\{9-MeAd(-H)\}]_n^{n+}$ in which binding modes of the deprotonated nucleobase and nuclearity of resulting cations depend on the nature of L .⁵ To the best of our

Chart 2



N-(9-Methyl-1,9-dihydro-purin-6-ylidene)-acetamide

N-(1-Methyl-2-oxo-2,3-dihydro-1*H*-pyrimidin-4-ylidene)-acetamide

knowledge, the reversible insertion of CH_3CN into a metal–nitrogen bond has been reported only in some tetranuclear Ir_2Ag_2 pyrazolyl amidine complexes.⁶

Moreover, in this Article we show that the insertion of CH_3CN does not occur in platinum nucleobase compounds stabilized by PMe_3 and PMe_2Ph ligands. It turns out that the adenine complexes $cis-[(PMe_3)_2Pt\{9-MeAd(-H)\}]_2^{2+}$ and $cis-[(PMe_2Ph)_2Pt\{9-MeAd(-H)\}]_3^{3+}$, previously characterized,^{7,8} can be prepared in acetonitrile and are indefinitely stable in this solvent, even at high temperature. Similarly, in the reaction of $cis-[(PMe_2Ph)_2Pt(\mu-OH)]_2(NO_3)_2$ with 1-MeCy in CH_3CN , the deprotonation of the nucleobase affords the trinuclear species $cis-[(PMe_2Ph)_2Pt\{1-MeCy(-H)\}]_3(NO_3)_3$ which does not react further with the solvent. Insertion reactions of the acetonitrile $C\equiv N$ group into metal–nucleobase bonds have been previously reported for a rhenium (IV)–adenine complex.⁹

Experimental Section

Instrumentation and Materials. 1H , ^{13}C , and ^{31}P NMR spectra were recorded on a Bruker AVANCE 300 spectrometer (at 300.13, 75.47, and 121.49 MHz, respectively), equipped with a variable temperature apparatus and were calibrated against the residual signals of the solvent (for 1H and ^{13}C) and external H_3PO_4 for ^{31}P . 1H , ^{15}N heterocorrelation experiments were performed on a Bruker 400 MHz spectrometer, and ^{15}N resonances were calibrated with nitromethane. The solvents CD_2Cl_2 , CD_3CN , and $CH_3^{13}CN$ (Aldrich) were distilled from CaH_2 .

Reagent grade chemicals were used as received unless otherwise stated. $cis-[(PMe_3)_2Pt(\mu-OH)]_2(ClO_4)_2$,² (**Caution: Perchlorates are potential explosives!**) $cis-[(PMe_2Ph)_2Pt(\mu-OH)]_2(NO_3)_2$,⁷ $cis-[(PMePh_2)_2Pt(\mu-OH)]_2(NO_3)_2$,¹⁰ and 9-MeAd¹¹ were synthesized as previously reported.

Synthetic Work. 1. $cis-[(PPh_3)_2Pt(\mu-OH)]_2(NO_3)_2$ (**1b**). The complex was prepared following the procedure described for the synthesis of the $PMePh_2$ analogue, with a yield of 69%.¹⁰ Elemental Anal. Calcd for $C_{36}H_{31}NO_4P_2Pt$: C, 54.14; H, 3.91; N, 1.75.

(2) Longato, B.; Bandoli, G.; Mucci, A.; Schenetti, L. *Eur. J. Inorg. Chem.* **2001**, 3021–3029.

(3) Broder, C. K.; Goeta, A. E.; Howard, A. K.; Hughes, A. K.; Johnson, A. L.; Malget, J. M.; Wade, K. *J. Chem. Soc., Dalton Trans.* **2000**, 3526–3533.

(4) Segerer, U.; Blaurock, S.; Sieler, J.; Hey-Hawkins, E. *Organometallics* **1999**, *18*, 2838–2842.

(5) Longato, B.; Pasquato, L.; Mucci, A.; Schenetti, L.; Zangrando, E. *Inorg. Chem.* **2003**, *42*, 7861–7871.

(6) Carmona, D.; Ferrer, J.; Lahoz, F. J.; Oro, L. A.; Lamata, M. P. *Organometallics* **1996**, *15* (5), 5175–5178.

(7) Schenetti, L.; Mucci, A.; Longato, B. *J. Chem. Soc., Dalton Trans.* **1996**, 299–303.

(8) Longato, B.; Pasquato, L.; Mucci, A.; Schenetti, L. *Eur. J. Inorg. Chem.* **2003**, 128–137.

(9) Pearson, C.; Beauchamp, A. L. *Inorg. Chem.* **1998**, *37*, 1242–1248.

(10) Longato, B.; Bandoli, G.; Dolmella, A. *Eur. J. Inorg. Chem.* **2004**, 1092–1099.

(11) Talman, E. G.; Brüning, W.; Reedijk, J.; Spek, A. L.; Veldman, N. *Inorg. Chem.* **1997**, *36*, 854–861.

Table 1. Crystal Data and Details of Refinements for Compounds **3a**, **3b**, and **5a**

	3a	3b	5a
formula	C ₃₄ H ₃₅ N ₇ O ₃ Pt	C ₄₄ H ₃₉ N ₇ O ₃ Pt	C ₃₃ H ₃₅ N ₅ O ₄ Pt
fw	846.72	970.85	822.69
crystal syst	triclinic	triclinic	orthorhombic
space group	<i>P</i> $\bar{1}$	<i>P</i> $\bar{1}$	<i>Pna</i> 2 ₁
<i>a</i> (Å)	10.236(2)	9.741(2)	14.933(4)
<i>b</i> (Å)	11.563(2)	12.303(3)	18.888(4)
<i>c</i> (Å)	16.510(3)	17.180(3)	11.860(3)
α (°)	107.79(3)	95.95(3)	90.0
β (°)	93.34(3)	96.78(3)	90.0
γ (°)	110.22(3)	105.30(3)	90.0
vol (Å ³)	1716.40(6)	1952.4(7)	3345.2(14)
Z	2	2	4
<i>D</i> _{calcd} (g cm ⁻³)	1.638	1.651	1.634
λ Mo K α (mm ⁻¹)	4.226	3.727	4.335
<i>F</i> (000)	840	968	1632
unique reflns	6014	8422	9157
reflns <i>I</i> > 2 σ (<i>I</i>)	4370	3614	6823
refined params	424	512	406
GOF	0.903	0.965	0.906
Flack param			0.016(6)
R1 (<i>I</i> > 2 σ (<i>I</i>)) ^a	0.0398	0.0455	0.0322
wR2 ^b	0.0667	0.0652	0.0667
max residuals (e/Å ³)	1.017	0.673	0.476

$$^a R1 = \sum ||F_o| - |F_c|| / \sum |F_o|. \quad ^b wR2 = [\sum w(F_o^2 - F_c^2)^2 / \sum w(F_o^2)^3]^{1/2}.$$

Found: C, 53.69; H, 3.84; N, 1.82. ¹H NMR in CDCl₃: 2.12 (br s, 1 H, OH); 7.55–7.11 (cm, 30 H, Ph). {¹H}³¹P NMR in CDCl₃: singlet at δ 8.45 (¹*J*_{Pt} = 3713 Hz). These spectroscopic data compare well with those of the BF₄ analogue.¹²

2. cis-[(PMePh₂)₂PtNH=C(Me){9-MeAd(-2H)}]NO₃ (3a**).** A suspension of *cis*-[(PMePh₂)₂Pt(μ -OH)]₂(NO₃)₂, **1a**, (716 mg, 0.5 mmol) and 9-MeAd (158 mg, 1.1 mmol) in CH₃CN (26 mL) was stirred for ca. 1 h, and the resulting pale yellow solution was heated at 50 °C for 12 h. A trace amount of metallic platinum was removed by filtration, and the solution was left to evaporate at room temperature. In 2–3 days pale yellow crystals, suitable for the X-ray analysis, were formed, which were separated from the solution and dried under vacuum (ca. 20 mg). Addition of Et₂O (25 mL) to the remaining solution caused the precipitation of a very pale yellow solid which was collected by filtration, washed with Et₂O, and dried under vacuum. The recovered solid (600 mg) was purified by dissolution in CH₃CN and precipitated by addition of diethyl ether. The yield of pure **3a** (pale yellow microcrystals) was 69%. Elemental Anal. Calcd for C₃₄H₃₅N₇O₃Pt: C, 48.23; H, 4.17; N, 11.58. Found: C, 48.20; H, 4.10; N, 11.48. ¹H and ¹⁵N NMR data are collected in Tables 3 and 4, respectively. {¹H}³¹P NMR in CD₃CN: AB multiplet at δ -3.36 (¹*J*_{Pt} = 3172 Hz) and -4.01 (¹*J*_{Pt} = 3265 Hz) with ²*J*_{PP} = 27.4 Hz. {¹H}¹³C NMR (in CD₃CN): (9-MeAd resonances) 156.18 (d, ³*J*_{CP} = 8.5 Hz, C-2), 150.42 (s, C-6), 149.56 (s, C-4), 144.16 (s, C-8), 30.05 (s, NCH₃). PMePh₂ resonances: 133.24 (d, ³*J*_{CP} = 10.3 Hz, C-2 and C-6), 133.05 (d, ²*J*_{CP} = 10.7 Hz, C-2', C-6'), 132.89 (d, ⁴*J*_{CP} = 2.5 Hz, C-4), 132.11 (d, ⁴*J*_{CP} = 2.3 Hz, C-4'), 129.84 (d, ³*J*_{CP} = 11.1 Hz, C-3 and C-5), 129.54 (d, *J*_{CP} = 10.8 Hz, C-3 and C-5), 128.47 (dd, *J*_{CP} = 60.0 and 3.5 Hz, C-1), 126.80 (dd, *J*_{CP} = 63.3 and 3.5 Hz, C-1), 14.41 (dd, *J*_{CP} = 44.4 and 3.5 Hz, PCH₃), 12.82 (dd, ¹*J*_{CP} = 45.8 and 3.7 Hz, PCH₃). CH₃CN resonances: 164.96 (s, ²*J*_{Cp} = 12 Hz). {¹H}³¹P NMR in CDCl₃: AB multiplet at δ -3.21 (¹*J*_{Pt} = 3173 Hz) and -3.50 (¹*J*_{Pt} = 3215 Hz) with ²*J*_{PP} = 27.4 Hz. {¹H}³¹P NMR in

Table 2. Selected Bond Lengths (Å) and Angles (Deg) in the Cation of **3a** and **3b**

	3a	3b
Pt–N(1)	2.115(5)	2.124(7)
Pt–N(2)	2.017(5)	2.011(7)
Pt–P(1)	2.290(2)	2.311(3)
Pt–P(2)	2.267(2)	2.281(3)
N(2)–C(3)	1.292(7)	1.279(11)
C(3)–C(7)	1.523(9)	1.509(11)
N(6)–C(3)	1.335(8)	1.358(11)
N(6)–C(6)	1.355(8)	1.319(9)
N(1)–C(2)	1.365(8)	1.349(9)
N(1)–C(6)	1.357(7)	1.397(10)
N(1)–Pt–N(2)	85.1(2)	84.4(3)
N(1)–Pt–P(1)	95.08(15)	93.04(19)
N(1)–Pt–P(2)	172.31(15)	173.5(2)
N(2)–Pt–P(1)	172.43(18)	176.3(3)
N(2)–Pt–P(2)	88.17(16)	89.4(2)
P(1)–Pt–P(2)	92.05(7)	93.08(10)
C(6)–N(1)–C(2)	118.6(6)	119.8(8)
C(6)–N(1)–Pt	122.5(4)	119.1(5)
C(2)–N(1)–Pt	118.9(4)	120.1(6)
C(3)–N(2)–Pt	127.1(5)	128.6(7)
N(2)–C(3)–N(6)	128.0(6)	126.5(8)
N(2)–C(3)–C(7)	117.3(6)	119.6(9)
N(6)–C(3)–C(7)	114.7(6)	113.9(8)
C(3)–N(6)–C(6)	122.4(6)	123.1(8)
N(1)–C(6)–N(6)	127.3(6)	127.7(8)
N(1)–C(6)–C(5)	116.1(6)	113.5(8)
N(6)–C(6)–C(5)	116.6(6)	118.7(8)

DMSO-*d*₆: AB multiplet at δ -3.05 (¹*J*_{Pt} = 3182 Hz) and -3.62 (¹*J*_{Pt} = 3264 Hz) with ²*J*_{PP} = 26.8 Hz.

3a, dissolved in a mixture of CD₃CN and CH₃¹³CN (2:1 v/v), exchanges the inserted CH₃CN molecule in a few hours at room temperature, as shown by the appearance of a ¹³C resonance at 164.3 ppm, flanked by poorly resolved ¹⁹⁵Pt satellites (²*J*_{Cp} ca. 12 Hz).²²

3. cis-[(PPh₃)₂PtNH=C(Me){9-MeAd(-2H)}]NO₃ (3b**).** A suspension of *cis*-[(PPh₃)₂Pt(μ -OH)]₂(NO₃)₂, **1b**, (211 mg, 0.132 mmol) and 9-MeAd (40 mg, 0.27 mmol) in CH₃CN (5 mL) was stirred for 2 h at ca. 25 °C. Addition of Et₂O (20 mL) to the resulting solution afforded a pale yellow solid which was purified by dissolution in hot CH₃CN, filtered to eliminate trace amounts of undissolved material, and precipitated with Et₂O. The pale yellow solid was collected by filtration, washed with Et₂O, and dried under vacuum. The yield of pure **3b** was 169 mg, yield 65%. Small crystals, suitable for single-crystal X-ray diffraction, were obtained by vapor diffusion of Et₂O into a CH₃CN solution of **3b**. Elemental Anal. Calcd for C₄₄H₃₉N₇O₃Pt: C, 54.43; H, 4.05; N, 10.10. Found: C, 53.42; H, 3.77; N, 10.08. {¹H}³¹P NMR in CD₃CN: AB multiplet at δ 10.27 (¹*J*_{Pt} = 3398 Hz) and 11.47 (¹*J*_{Pt} = 3269 Hz) with ²*J*_{PP} = 24.5 Hz. Inverse-detected ¹³C NMR (in DMSO-*d*₆): (9-MeAd resonances) 155.5 (C-2), 148.3 (C-4), 125.2 (C-5), 149.0 (C-6), 144.1 (C-8), 29.4 (NCH₃). PPh₃ resonances: 133.2–126.8. CH₃CN resonances: δ 163.0 and 27.0. {¹H}³¹P NMR in CDCl₃: AB multiplet at δ 11.33 (¹*J*_{Pt} = 3385 Hz) and 10.86 (¹*J*_{Pt} = 3369 Hz) with ²*J*_{PP} = 24.7 Hz. {¹H}³¹P NMR in DMSO-*d*₆: AB multiplet at δ 10.91 (¹*J*_{Pt} = 3260 Hz) and 9.47 (¹*J*_{Pt} = 3428 Hz) with ²*J*_{PP} = 24.6 Hz.

4. cis-[(PMePh₂)₂PtNH=C(Me){1-MeCy(-2H)}]NO₃ (5a**).** A suspension of **1a** (233 mg, 0.17 mmol) and 1-MeCy (44 mg, 0.3 mmol) in CH₃CN (7 mL) was stirred at room temperature for 30 min. Addition of Et₂O to the resulting pale yellow solution afforded a white solid which was separated by filtration and recrystallized from CH₃CN/Et₂O. The yield of pure **5a** was 230 mg (yield 81%). Elemental Anal. Calcd for C₃₃H₃₅N₅O₄Pt: C, 48.18; H, 4.29; N,

(12) (a) Bushnell, G. W.; Dixon, K. R.; Hunter, R. G.; McFarland, J. J. *Can. J. Chem.* **1972**, *50*, 3694–3699. (b) Li, J. J.; Li, W.; James, A. J.; Holbert, T.; Sharp, T.; Sharp, P. R. *Inorg. Chem.* **1999**, *38*, 1563–1572.

Table 3. ^1H NMR Data (δ in ppm, J in Hz) for Complexes **3a** and **3b** in Various Solvents and Temperatures

compound	solvent (°C)	H(2)	H(8)	NH	NCH ₃	N=CCH ₃	PMe	Ph
3a	DMSO- <i>d</i> ₆ (25)	8.16 app t ($^4J_{\text{HP}} = 1.8$)	8.03 s	5.84 br s	3.52 s	2.01 s	2.23 d ($^2J_{\text{HP}} = 10.0$) 1.91 d ($^2J_{\text{HP}} = 9.5$)	7.64–7.28
3a	CD ₃ CN (25)	8.05 app t ($^4J_{\text{HP}} = 1.7$; $^3J_{\text{HPt}} = 17.1$)	7.87 s	5.39 br s	3.51 s	1.98 s	2.01 d ($^2J_{\text{HP}} = 10.2$) 1.81 d ($^2J_{\text{HP}} = 9.6$)	7.66–7.30
3a	CD ₃ CN (–40)	7.94 app t ($^4J_{\text{HP}} = 1.8$)	7.89 s	5.36 app dd ($^3J_{\text{HP}} = 4–6$)	3.45 s	1.92 s	1.97 d ($^2J_{\text{HP}} = 8.7$) 1.76 d ($^2J_{\text{HP}} = 9.3$)	7.64–7.22
3a	CDCl ₃ (25)	7.85 s	8.12 s	5.38 br s	3.62 s	2.07 s	2.17 d ($^2J_{\text{HP}} = 9.2$) 1.83 ($^2J_{\text{HP}} = 8.6$)	7.64–7.28
3b	DMSO- <i>d</i> ₆ (25)	8.08 app t ($^4J_{\text{HP}} = 1–2$)	8.17 s	6.11 dd ($^3J_{\text{HP}} = 3–7$)	3.54 s	1.87 s		7.64–7.14
3b	CD ₃ CN (25)	8.08 app t ($^4J_{\text{HP}} = 1.8$; $^3J_{\text{HPt}} = 18$)	7.86 s	5.69 br s	3.46 s	1.89 s		7.61–7.17
3b	CD ₃ CN (–40)	7.94 app t ($^4J_{\text{HP}} = 1.8$)	7.62 s	5.93 app dd ($^3J_{\text{HP}} = 5.3$)	3.42 s	1.86 s		7.50–7.16
3b	CDCl ₃ (25)	8.11 app t ($^4J_{\text{HP}} = 1.5$)	7.81 s	5.44 br s	3.50 s	1.87 s		7.61–7.17

Table 4. ^{15}N NMR Data (δ in ppm, J in Hz) for Complexes **3a, b, 2a**, and **4b** in DMSO-*d*₆

complex	N(1)	N(3)	N(6)	N(7)	N(9)	CH ₃ CN
3a	–198.0 ($^2J_{\text{NP}} = 39$)	–138.6	–172.1	–127.1	–220.8	–233.5 ($^2J_{\text{NP}} = 53$)
3b	–200.0 ($^2J_{\text{NP}} = 60$)	–138.8	–172.0	–126.7	–221.0	–234.5 ($^2J_{\text{NP}} = 58$)
2a	–132.0	–155.3	–244.7 ($^2J_{\text{NP}} = 50$)	–190.4 ($^2J_{\text{NP}} = 60$)	–217.8	
4b	–131.5	–153.2	–243.1 ($^2J_{\text{NP}} = 56$)	–191.5	–216.5	

Table 5. Selected Bond Lengths (Å) and Angles (Deg) in the Cation of **5a**

Pt–N(3)	2.097(4)	N(3)–C(4)	1.358(7)
Pt–N(2)	2.036(4)	N(3)–C(2)	1.388(6)
Pt–P(1)	2.279(1)	N(4)–C(3)	1.337(7)
Pt–P(2)	2.262(1)	N(4)–C(4)	1.356(7)
N(2)–C(3)	1.295(7)	C(3)–C(7)	1.503(8)
N(2)–Pt–N(3)	83.12(19)	C(2)–N(3)–C(4)	120.9(4)
N(2)–Pt–P(1)	169.24(14)	C(2)–N(3)–Pt	117.8(3)
N(2)–Pt–P(2)	88.93(15)	C(4)–N(3)–Pt	121.3(4)
N(3)–Pt–P(1)	95.60(12)	N(2)–C(3)–N(4)	126.7(5)
N(3)–Pt–P(2)	172.00(12)	N(2)–C(3)–C(7)	118.7(5)
P(1)–Pt–P(2)	92.37(5)	N(4)–C(3)–C(7)	114.6(5)
C(3)–N(2)–Pt	124.9(4)	N(3)–C(4)–N(4)	125.6(5)
C(3)–N(4)–C(4)	122.6(5)	N(3)–C(4)–C(5)	117.8(5)
		N(4)–C(4)–C(5)	116.6(5)

8.51. Found: C, 48.01; H, 4.08; N, 8.47. ^1H NMR data are collected in Table 6. $\{^1\text{H}\}^{31}\text{P}$ NMR in CD₂Cl₂ at 27 °C: AB multiplet at δ –6.06 ($^1J_{\text{Ppt}} = 3325$ Hz) and –9.43 ($^1J_{\text{Ppt}} = 3311$ Hz) with $^2J_{\text{PP}} = 27.2$ Hz; at –40 °C, AB multiplet at δ –4.65 ($^1J_{\text{Ppt}} = 3280$ Hz) and –6.00 ($^1J_{\text{Ppt}} = 3270$ Hz) with $^2J_{\text{PP}} = 28.1$ Hz and AX multiplet at δ –7.15 ($^1J_{\text{Ppt}} = 3330$ Hz) and –13.05 ($^1J_{\text{Ppt}} = 3330$ Hz) with $^2J_{\text{PP}} = 26.4$ Hz, with relative intensities 1.2:1, respectively. $\{^1\text{H}\}^{13}\text{C}$ NMR (in CD₂Cl₂ at 27 °C): 165.75 (s, CH₃CN), 161.45 (s, C-4), 155.21 (s, C-2), 144.37 (s, C-6), 104.22 (d, $^4J_{\text{CP}} = 3.5$ Hz, C-5), 37.81 (s, NCH₃); 133.0–125.5 (complex multiplets, PMePh₂), 12.39 (d, $^1J_{\text{CP}} = 42.7$ Hz, PMePh₂). $\{^1\text{H}\}^{31}\text{P}$ NMR in CD₃CN at 27 °C: AB multiplet at δ –5.86 (d, $^2J_{\text{PP}} = 27.2$ Hz, $^1J_{\text{Ppt}} = 3350$ Hz) and –8.80 (s, $^1J_{\text{Ppt}} = 3345$ Hz); at –40 °C, AB multiplet (relative

intensity 58%) at δ –4.34 ($^1J_{\text{Ppt}} = 3290$ Hz), –5.33 ($^1J_{\text{Ppt}} = 3280$ Hz) with $^2J_{\text{PP}} = 28.4$ Hz and AX multiplet (relative intensity 42%) at δ –6.31 ($^1J_{\text{Ppt}} = 3360$ Hz), –11.16 ($^1J_{\text{Ppt}} = 3360$ Hz) with $^2J_{\text{PP}} = 26.4$ Hz. $\{^1\text{H}\}^{31}\text{P}$ NMR in DMSO-*d*₆ at 27 °C: AB multiplet at δ –5.38 (d, $^2J_{\text{PP}} = 26.7$ Hz, $^1J_{\text{Ppt}} = 3334$ Hz) and –8.38 (s, $^1J_{\text{Ppt}} = 3310$ Hz). In a second experiment, carried out in CD₃CN (0.5 mL), a suspension of 44 mg of **1a** and 1-MeCy (8.1 mg) was stirred for 1 h, at room temperature. The resulting pale yellow solution, after 24 h, separated pale yellow crystals of **5a** (ca. 30 mg) which were used for the X-ray analysis.

5. cis-[(PPh₃)₂PtNH=C(Me){1-MeCy(–2H)}]NO₃ (5b**).** A suspension of **1b** (81 mg, 0.05 mmol) and 1-MeCy (12.7 mg, 0.10 mmol) in CH₃CN (4 mL) was stirred at room temperature for 12 h. Addition of Et₂O to the resulting pale yellow solution afforded a pale yellow solid which was separated by filtration and recrystallized from CH₃CN/Et₂O. The yield of pure **5b** was 58 mg (yield 61%). Elemental Anal. Calcd for C₄₃H₃₉N₅O₄P₂Pt: C, 54.54; H, 4.16; N, 7.39. Found: C, 54.40; H, 4.10; N, 7.29. $\{^1\text{H}\}^{31}\text{P}$ NMR in CD₃CN at 27 °C: AB multiplet at δ 8.81 ($^1J_{\text{Ppt}} = 3476$ Hz) and 8.01 ($^1J_{\text{Ppt}} = 3432$ Hz) with $^2J_{\text{PP}} = 25.0$ Hz; in CDCl₃, AB multiplet at δ 8.99 ($^1J_{\text{Ppt}} = 3477$ Hz) and 7.77 ($^1J_{\text{Ppt}} = 3419$ Hz) with $^2J_{\text{PP}} = 24.8$ Hz; DMSO-*d*₆, AB multiplet at δ 9.48 ($^1J_{\text{Ppt}} = 3444$ Hz) and 8.45 ($^1J_{\text{Ppt}} = 3442$ Hz) with $^2J_{\text{PP}} = 25.0$ Hz.

6. Decomposition of 5a in Chlorinated Solvents. A solution of **5a** (139 mg) in CH₂Cl₂ (5 mL) was left at room temperature for 2 weeks. Addition of Et₂O afforded a white precipitate which was recovered by filtration, washed with Et₂O, and dried under vacuum. The elemental analysis of the solid (71 mg), after recrystallization from CH₂Cl₂/Et₂O, shows a composition significantly different from the values calculated for the expected cytosine complex [(PMePh₂)₂Pt{1-MeCy(–H)}]_n(NO₃)_n. Calcd for C₃₁H₃₂N₄O₄P₂Pt: C, 47.63; H, 4.13; N, 7.17. Found: C, 45.99; H, 4.13; N, 6.84. ^1H NMR in CDCl₃ at 27 °C (δ , ppm): (1-MeCy(–H)) 6.73 (d, $^3J_{\text{HH}} = 5.1$ Hz, 1 H, H(6)), 6.58 (s, 1 H, NH), 6.34 (d, $^3J_{\text{HH}} = 6.0$ Hz, 1 H, H(5)), 2.89 (s, 3 H, NCH₃); PMePh₂, 8.06–7.04 (cm 20 H, PPh), 2.75 (d, $^2J_{\text{HP}} = 10$ Hz, 3 H, PMe), 2.28 (br s, 3 H, PMe). $\{^1\text{H}\}^{31}\text{P}$ NMR in CDCl₃ at 27 °C: apparent doublet at δ –11.05 ($^2J_{\text{PP}} = 21$ Hz, $^1J_{\text{Ppt}} = 3356$ Hz) and an extremely broad resonance in the range

Table 6. ^1H NMR Data (δ in ppm, J in Hz) for Complexes **5a** and **5b** in Various Solvents and Temperatures

compound	solvent T ($^{\circ}\text{C}$)	H(5)	H(6)	NH	NCH_3	$\text{N}=\text{CCH}_3$	PMe	Ph
5a	DMSO- d_6 (25)	5.84 dd ($^3J_{\text{HH}} = 7.1$; $^5J_{\text{HP}} = 1.3$)	7.27 d ($^3J_{\text{HH}} = 7.1$)	6.29 br s	3.62 s	1.95 s	2.13 d ($^2J_{\text{HP}} = 10.8$)	7.64–7.28
5a	CD_3CN (25)	5.81 dd ($^3J_{\text{HH}} = 7.1$; $^5J_{\text{HP}} = 1.4$)	6.93 d ($^3J_{\text{HH}} = 7.1$)	5.50 br s	2.56 s	1.89 s	ca. 2 br s 1.89 d ($^2J_{\text{HP}} = 10.5$) 1.93 d ($^2J_{\text{HP}} = 10.0$)	7.60–7.29
5a	CD_2Cl_2 (25)	5.91 dd ($^3J_{\text{HH}} = 7.2$; $^5J_{\text{HP}} = 1.5$)	7.92 d ($^3J_{\text{HH}} = 7.2$)	5.53 br s	2.63 s	2.07 s	1.84 d ($^2J_{\text{HP}} = 10.0$) 1.93 d ($^2J_{\text{HP}} = 11.0$)	7.62–7.34
5b	DMSO- d_6 (25)	5.86 dd ($^3J_{\text{HH}} = 7$; $^5J_{\text{HP}} = 0.9$)	7.26 d ($^3J_{\text{HH}} = 7.3$)	7.03 app t ($^3J_{\text{HP}} = 4-6$)	3.50 s	1.85 s		7.67–7.28
5b	CD_3CN (25)	5.83 dd ($^3J_{\text{HH}} = 7.2$; $^5J_{\text{HP}} = 1.2$)	6.91 d ($^3J_{\text{HH}} = 7.2$)	5.84 br s	2.49 s	1.95 s		7.80–7.23
5b	CDCl_3 (25)	6.02 dd ($^3J_{\text{HH}} = 7.0$; $^5J_{\text{HP}} = 1.5$)	7.20 d ($^3J_{\text{HH}} = 7.1$)	5.72 br s	2.71 s	1.92 s		7.69–7.27

of -5 to -10 ppm. Similar data were obtained in CD_3CN , even after several days at 45 $^{\circ}\text{C}$, indicating that the isolated solid does not react with the solvent.

7. Reaction of $cis\text{-}[\text{L}_2\text{Pt}(\mu\text{-OH})_2]^{2+}$ ($\text{L} = \text{PMe}_3, \text{PMe}_2\text{Ph}$) with 9-MeAd and 1-MeCy in Acetonitrile. A suspension of $cis\text{-}[(\text{PMe}_3)_2\text{Pt}(\mu\text{-OH})_2](\text{ClO}_4)_2$ (46 mg, 0.05 mmol) and 9-MeAd (15 mg, 0.1 mmol) in 1 mL of CD_3CN was stirred at room temperature for 4 h obtaining a colorless solution. The ^{31}P NMR of the reaction mixture showed the presence of two AB multiplets, flanked by ^{195}Pt satellites, at $\delta -27.34$ ($^1J_{\text{PPt}} = 3260$ Hz) and -28.56 ($^1J_{\text{PPt}} = 3117$ Hz, $^2J_{\text{PP}} = 25.1$ Hz) ppm and $\delta -29.66$ ($^1J_{\text{PPt}} = 3021$ Hz) and -30.86 ($^1J_{\text{PPt}} = 3218$ Hz, $^2J_{\text{PP}} = 26.1$ Hz) ppm, with relative intensities ca. 5:1, respectively. In 2 weeks at room temperature the first multiplet quantitatively converted in the second one, attributable to the dinuclear species $cis\text{-}[(\text{PMe}_3)_2\text{Pt}\{9\text{-MeAd}(-\text{H})\}]_2(\text{ClO}_4)_2$. The solution was then heated at 50 $^{\circ}\text{C}$ for 5 days. Further changes on the ^{31}P NMR spectrum were not observed. Addition of Et_2O afforded a white precipitate which was recovered by filtration and dried under vacuum to give 25 mg of solid which was further characterized by elemental analysis, mass spectrometry, and NMR spectroscopy. Anal. Calcd for $\text{C}_{12}\text{H}_{24}\text{N}_5\text{ClO}_4\text{P}_2\text{Pt}$: C, 24.23; H, 4.07; N, 11.77. Found: C, 24.17; H, 4.01; N, 11.69. ESI mass spectrum in CH_3CN : m/z 1089 due to the monovalent cation $[(\text{PMe}_3)_2\text{Pt}\{9\text{-MeAd}(-\text{H})\}]_2(\text{ClO}_4)^+$. ^1H and $\{^1\text{H}\}^{31}\text{P}$ NMR data (in DMSO- d_6) of the isolated complex were in agreement those reported for $cis\text{-}[(\text{PMe}_3)_2\text{Pt}\{9\text{-MeAd}(-\text{H})\}]_2(\text{NO}_3)_2$.⁷ With similar procedures, complexes $cis\text{-}[(\text{PMe}_2\text{Ph})_2\text{Pt}\{9\text{-MeAd}(-\text{H})\}]_3(\text{NO}_3)_3$ and $cis\text{-}[(\text{PMe}_2\text{Ph})_2\text{Pt}\{1\text{-MeCy}(-\text{H})\}]_3(\text{NO}_3)_3$ ¹³ were prepared reacting $cis\text{-}[(\text{PMe}_2\text{Ph})\text{Pt}(\mu\text{-OH})_2](\text{NO}_3)_2$ with 9-MeAd and 1-MeCy, respectively, in CH_3CN . No reaction with the solvent was observed, even at 50 $^{\circ}\text{C}$ within 1 week.

X-ray Structure Determinations. Diffraction data were collected on a Stoe & Cie diffractometer equipped with a STADI4 CCD detector (compounds **3a,b**) and on a Nonius DIP-1030H system (**5a**) graphite-monochromatized Mo $K\alpha$ radiation. Cell refinement, indexing, and scaling of the data sets were carried out using the program X-RED¹⁴ (compounds **3a,b**) and by programs Denzo and Scalepack for **5a**.¹⁵ The structures were solved by direct methods (SHELX86 and SHELXTL NT) and Fourier analyses and

were refined by the full-matrix least-squares method based on F^2 with all observed reflections.¹⁶ In **3b** the nitrate oxygen atoms were found disordered over two positions with occupancy factors refined at 0.43(2) and 0.57(2). The final cycles with fixed contribution of hydrogen atoms at calculated positions converged to final R1 and wR2 factors reported in Table 1.

All the calculations were performed using the WinGX System, version 1.64.05.¹⁷

Results and Discussion

Synthesis and Characterization of $cis\text{-}[\text{L}_2\text{PtNH}=\text{C}(\text{Me})\{9\text{-MeAd}(-2\text{H})\}]\text{NO}_3$ ($\text{L} = \text{PMePh}_2$, **3a; PPh_3 , **3b**).** We have recently shown that the hydroxo complex $cis\text{-}[(\text{PMePh}_2)_2\text{Pt}(\mu\text{-OH})_2](\text{NO}_3)_2$, **1a**, reacts with the 9-substituted methyladenine (9-MeAd) to give the cyclic trimer $cis\text{-}[(\text{PMePh}_2)_2\text{Pt}\{9\text{-MeAd}(-\text{H})\}]_3(\text{NO}_3)_3$, **2a**, containing the NH_2 -deprotonated adenine bridging the metal centers through the N(1) and N(6) atoms.⁵ When the reaction is carried out in CH_3CN , the initially formed complex **2a**, slowly converts into the mononuclear species $cis\text{-}[(\text{PMePh}_2)_2\text{PtNH}=\text{C}(\text{Me})\{9\text{-MeAd}(-2\text{H})\}]\text{NO}_3$, **3a**, according to the reaction shown in Scheme 1.

In the same experimental conditions, complex **1b** forms immediately the insertion product $cis\text{-}[(\text{PPh}_3)_2\text{PtNH}=\text{C}(\text{Me})\{9\text{-MeAd}(-2\text{H})\}]\text{NO}_3$, **3b**. Both the complexes have been isolated in fairly good yield. X-ray analyses of **3a,b** show that the insertion of a CH_3CN molecule into the adenine Pt–N(6) bond had occurred, with formation of a six atoms metalocycle, as depicted in Figures 1 and 2, respectively.

A selection of bond distances and angles for these structures is collected in Table 2, indicating a close similarity

(13) Longato, B.; Montagner, D.; Zangrando, E. Manuscript in preparation.

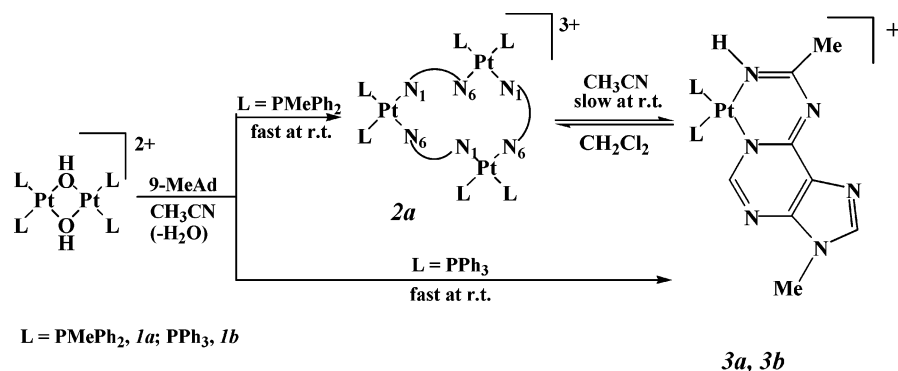
(14) X-RED, version 1.22; Stoe & Cie: Darmstadt, Germany, 2001.

(15) Otwinowski, Z.; Minor, W. Processing of X-ray Diffraction Data Collected in Oscillation Mode. In *Methods in Enzymology*; Carter, C. W., Jr., Sweet, R. M., Eds; Macromolecular Crystallography, Part A; Academic Press: New York, 1997; Vol. 276, pp 307–326.

(16) (a) Sheldrick, G. M. SHELXTL, NT, version 5.10; Bruker Analytical X-ray System: Madison WI, 1999. (b) Sheldrick, G. M. SHELX97 Programs for Crystal Structure Analysis, release 97-2; University of Göttingen: Göttingen, Germany, 1998.

(17) Farrugia, L. J. *J. Appl. Crystallogr.* **1999**, *32*, 837–838.

Scheme 1



of the metal coordination sphere in the two adducts. The platinum is bound to the nucleobase at the N(1) site, to the inserted acetonitrile nitrogen N(2), and completes the square planar coordination through phosphorus donors. The Pt–N(1) bond lengths are 2.115(5), 2.124(7) Å, in **3a** and **3b**, respectively, while Pt–N(2), of 2.017(5) and 2.011(7) Å, are slightly shorter. The Pt–P bond distances average to 2.287(2) Å, a value comparable to that found in the parent complex **2a** (2.280(4) Å).⁵ The coordination N₂P₂ donors show a slight tetrahedral distortion in **3a**, with deviations of ca. ±0.10 Å from its mean plane, while they are coplanar in **3b**, with the Pt ion slightly displaced by 0.04 Å in both complexes. Figure 3 displays a side view along the P(1)–P(2) vector in **3a** (a similar conformation is also exhibited by **3b**), showing the bending orientation assumed by the adenine–acetonitrile moiety with respect to the coordination plane. The dihedral angle formed by the mean planes through these atoms is of 29.2(2)° and 34.7(2)°, in **3a** and **3b**, respectively. The metal displacement from the plane defined by N(1)/C(6)/C(3)/N(2) is of 0.52 and 0.65 Å in the two complexes.

In all the structures reported the H atom at acetonitrile nitrogen N(2) was included considering the evidences achieved from ¹H, ¹⁵N NMR experiments, since the electron density maps did not allow us to definitely locate this hydrogen atom. The values of bond distance inside the chelating unit (Table 2) indicate a significant π electron delocalization, similar to that found in a related platinum(II) metallacycle.¹⁸ In particular, the C(3)–N(2) bond distances for the inserted CH₃CN molecule present a value typical for a double bond,¹⁹ being of 1.292(7) and 1.279(11) Å in **3a** and **3b**, respectively. In the C(3)–N(6)–C(6)–N(1)–C(2) fragment the distances are slightly longer varying in a range from 1.335(8) to 1.397(10) Å. All other bond lengths and angles inside the nucleobase are in the usual range.²⁰ Compound **3b** shows an intramolecular phenyl stacking occurring between rings of ipso carbon C(1c) and C(1d).

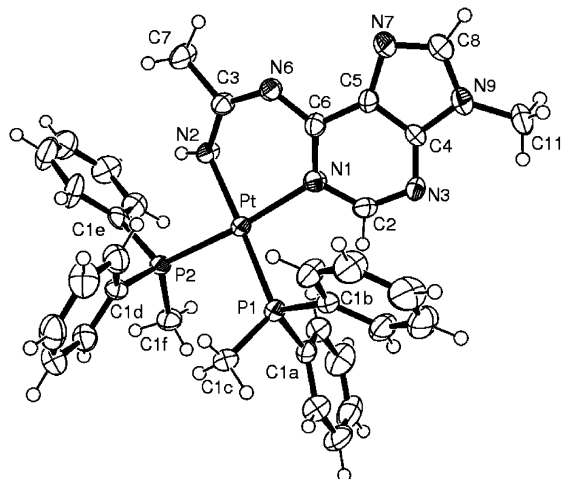


Figure 1. ORTEP drawing (ellipsoid 40% probability level) of the cation of **3a**.

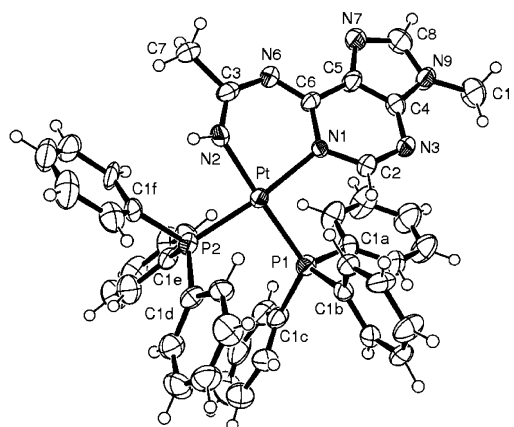


Figure 2. ORTEP drawing (ellipsoid 40% probability level) of the cation of **3b**.

NMR Studies in Solution. The reaction with acetonitrile has been followed by NMR spectroscopy. Figure 4 shows the changes of the ³¹P NMR spectra of a CD₃CN solution of **2a** in the course of the transformation to **3a**.

A freshly prepared solution of **2a** (trace a) exhibits a sharp AB multiplet, flanked by the ¹⁹⁵Pt satellites, whose parameters are similar to those obtained in chlorinated solvents in which **2a** maintains the trinuclear structure found in the solid state.⁵ In several days at room temperature, the multiplet is replaced by a new AB multiplet at lower field, attributable

(18) Guedes da Silva, M.; Ferreira, C. M. P.; Branco, E. M. P. R. P.; Fraústo da Silva, J. J. R.; Pombeiro, A. J. L.; Michelin, R.; Belluco, U.; Bertani, R.; Mozzon, M.; Bombieri, G.; Benetollo, F.; Kukushkin, V. Y. *Inorg. Chim. Acta* **1997**, *265*, 267–270.

(19) Allen, F. H.; Kennard, O.; Watson, D. G.; Brammer, L.; Orpen, A. G. *J. Chem. Soc., Perkin Trans. 2* **1987**, S1.

(20) Velders, A. V.; van der Geest, B.; Kooijman, H.; Spek, A.; Haasnoot, J. G.; Reedijk, J. *Eur. J. Inorg. Chem.* **2001**, 369–372.

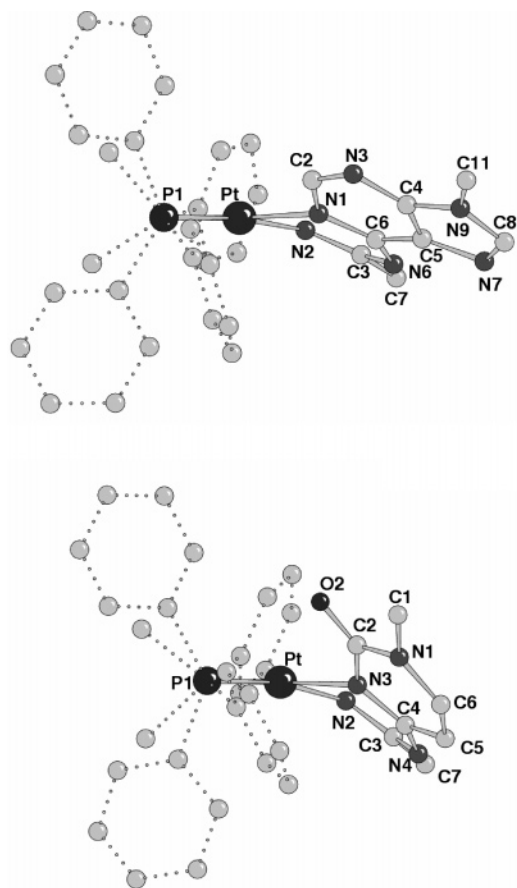


Figure 3. Perspective view of the complexes **3a** and **5a** along the P1–P2 direction showing the orientation of the nucleobase moiety with respect to the coordination plane.

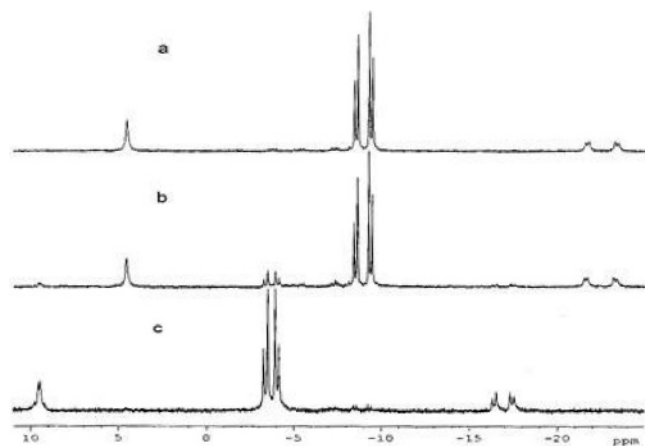
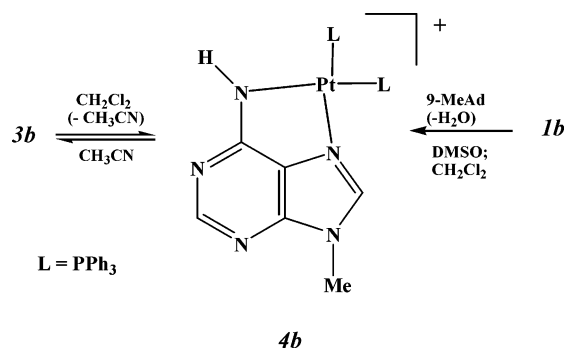


Figure 4. $^{31}\text{P}\{^1\text{H}\}$ NMR spectra of **2a** in CD_3CN at 27°C : (a) fresh solution; (b) after 24 h; (c) after 2 weeks at room temperature.

to complex **3a**. The reaction appears complete in 3 weeks (trace c), and no intermediates are detectable during the transformation (trace b).

The formation of **3a** causes a downfield shift of both the ^{31}P nuclei (ca. 5.2 ppm), whereas only one of the $^1J_{\text{PPt}}$ values changes significantly (from 3372 Hz in **2a** to 3265 Hz in **3a**). The resonance at -3.36 ppm, whose value of $^1J_{\text{PPt}}$ (3172 Hz) is very similar to one of those found in the parent complex **2a** (3192 Hz), can be attributed to the phosphine in trans to the adenine N(1) atom. The small change of $^1J_{\text{PPt}}$ for this phosphine reflects the invariance of the Pt–N(1) bond

Scheme 2



length found in the two complexes (Pt–N(1) = 2.117(10) Å (average)⁵ in **2a**, and 2.115(5) Å in **3a**).

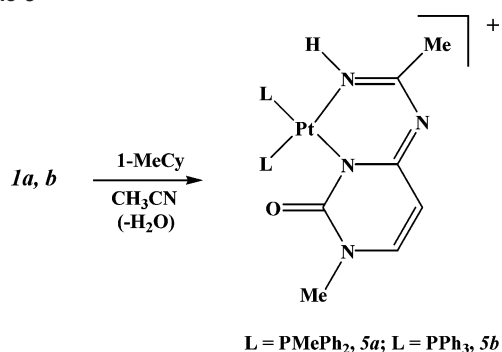
In the spectrum of **3a**, the methyl protons of the phosphines exhibit distinct and well-resolved resonances, in agreement with the chemical inequivalence of the two ligands. The ^1H NMR data, in various solvents and temperatures, are collected in Table 3.

For thorough ^1H and ^{13}C resonance assignments the routine 1- and 2-D NMR techniques have been employed. Discrimination between the adenine H(2) and H(8) protons was achieved by heteronuclear multiple bond correlations (HMBC) C/H experiments. Coordination of the adenine at the N(1) position is confirmed by the splitting of the resonances C(2) (δ 156.3, $^3J_{\text{CP}} = 8.5$ Hz) and H(2) (δ 8.16, $^4J_{\text{HP}} = 1.8$ Hz), due to the coupling with ^{31}P nuclei, in the $\{^1\text{H}\}^{13}\text{C}$ and ^1H spectra of **3a**. Moreover, HMBC ^{15}N , ^1H experiments show that the resonances at δ 5.84 in **3a** and 6.11 ppm in **3b** correlate with the ^{15}N resonances at δ -233.5 (**3a**) and -234.5 ppm (**3b**), indicating that the nitrogen atom of the inserted CH_3CN is protonated. The pertinent ^{15}N NMR data are collected in Tables 4, while the spectra are available as Supporting Information.

These attributions are in line with the observation that the NH resonance at δ 6.11 in **3b** occurs as a doublet of doublets, due to coupling with ^{31}P nuclei, separated by 3–7 Hz, typical values for three-bonds ^1H – ^{31}P interactions. Similarly, in **3a** the NH resonance is a broad singlet at ambient temperature but exhibits fine structure at -40°C (See Table 3). The process responsible of these changes with the temperature was not investigated in detail. However, the possible exchanges of the NH proton between the N(2) and the N(6) atoms for **3a** in $\text{DMSO}-d_6$ was ruled out through a ROESY experiment. The whole of these data supports the conclusion that the anionic ligand in **3a** and **3b**, abbreviated as $\text{NH}=\text{C}(\text{Me})\{9\text{-MeAd}(-2\text{H})\}$, is the deprotonated form of the amidine *N*-(9-methyl-1,9-dihydro-purin-6-ylidene)-acetamidine (see Chart 2).

In solution complexes **3a,b** are stable only in acetonitrile, in which the inserted CH_3CN molecule exchanges with the solvent (see experimental). In chlorinated solvents at room temperature, **3a** slowly releases the inserted CH_3CN molecule reforming the trinuclear species **2a** (Scheme 1). The reaction leads to an equilibrium mixture in ca. 4 weeks and, in a solution ca. 3.0×10^{-2} M (in CDCl_3) the relative intensities of the ^{31}P NMR signals of **2a** and **3a** are ca. 3:1. On the

Scheme 3



contrary, **3b** in CH_2Cl_2 (and DMSO) undergoes a complete decomposition with formation of the mononuclear species **4b** (Scheme 2) in which the NH_2 -deprotonated nucleobase chelates the metal center at the N(6), N(7) sites.²¹

The PMePh_2 analogue of this complex was previously characterized as the main component the mixture of products obtained when **2a** is dissolved in DMSO.⁵ Complex **4b** can be isolated as pure product by reacting **1b** with 9-MeAd in dichloromethane.²¹ In CH_3CN solution **4b** slowly regenerates **3b**, indicating a complete reversibility in the insertion reaction of acetonitrile.

Synthesis and Characterization of *cis*-[$\text{L}_2\text{PtNH}=\text{C}(\text{Me})\{1\text{-MeCy}(-2\text{H})\}]\text{NO}_3$ ($L = \text{PMePh}_2, \mathbf{5a}; L = \text{PPh}_3, \mathbf{5b}$). A similar metal-promoted coupling of CH_3CN with the exocyclic nitrogen of 1-methylcytosine (1-MeCy) is observed when complexes **1a,b** react with the nucleobase in acetonitrile (Scheme 3).

Mixtures of **1a** or **1b** and 1-MeCy (molar ratio 1:2) in CH_3CN , in a few hours at room temperature, form pale yellow solutions from which the compounds *cis*-[$\text{L}_2\text{PtNH}=\text{C}(\text{Me})\{1\text{-MeCy}(-2\text{H})\}]\text{NO}_3$ ($L = \text{PMePh}_2, \mathbf{5a}; L = \text{PPh}_3, \mathbf{5b}$) can be separated by crystallization (**5a**) or precipitation with Et_2O (**5b**). The NMR analysis of the reaction mixture, performed before the separation of the solid, showed the quantitative formation of **5b**, whereas for **5a** the yield was ca. 90%. The remaining product is a species, not yet completely characterized, that can be isolated when **5a** is dissolved in chlorinated solvents (see the Experimental Section).

The X-ray structure analysis of complex **5a** (Figure 5) shows the platinum bound to the phosphines and to the nitrogen donors of the adduct obtained from cytosine with a MeCN solvent molecule, the cytosine coordination site being N(3).

Both the Pt–P and Pt–N bond lengths are comparable to those measured in **3a** and **3b** within 2σ (Table 5). The P_2N_2 square planar geometry exhibits a slight tetrahedral distortion (atom displacement of about $\pm 0.10 \text{ \AA}$) with the P_2Pt and N_2Pt planes forming a dihedral angle of 10.7° . But more severe deformations are detected in the six-membered ring with Pt and N(4) located above the mean plane passing through N(2), C(3), C(4), and N(3) atoms by 0.78 and 0.13 Å , respectively. The latter plane forms an angle of 15.7° with

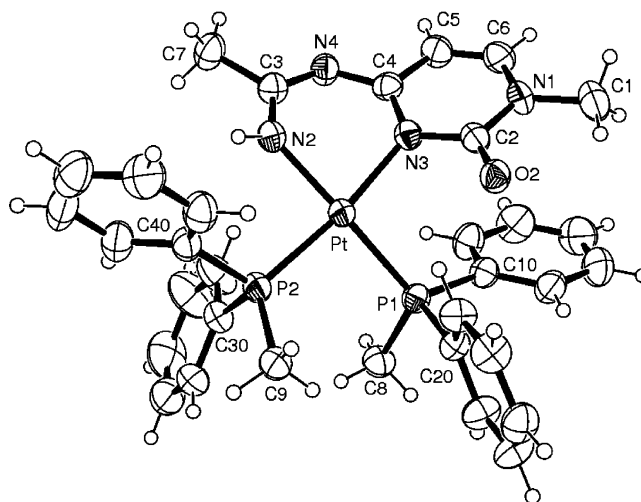


Figure 5. ORTEP drawing (ellipsoid 40% probability level) of the cation of **5a**.

the cytosine ring. The overall complex conformation, as well as the bond distances, are close to those detected in the adenine derivatives, indicating a similar geometry in the fragment resulting from the binding of the acetonitrile molecule to the exocyclic amino nitrogen N(4). The perspective view of **5a** (Figure 3) shows the orientation assumed by the chelating ligand with respect to the coordination plane (dihedral angle of $40.8(1)^\circ$).

The characterization of **5a,b** in solution was performed in CD_3CN , $\text{DMSO-}d_6$ and chlorinated solvents, and the pertinent ^1H NMR data are collected in Table 6.

The pyrimidinic protons occur as sharp doublets ($^3J_{\text{HH}} = 7.8 \text{ Hz}$), and that attributed to H(5) shows a further splitting due to the coupling with a ^{31}P nucleus ($^5J_{\text{HP}} = 1.3\text{--}1.5 \text{ Hz}$). The NH proton in **5a** exhibits a broad singlet (in $\text{DMSO-}d_6$), while in **5b** this signal has a fine structure (apparent triplet, $^3J_{\text{HP}} = 4\text{--}6 \text{ Hz}$) due to coupling with ^{31}P nuclei. This finding supports the protonation on the inserted acetonitrile nitrogen, as found in **3a** and **3b**. Thus, the anionic ligand in **5b** can be described as the deprotonated form of the amidine *N*-(1-methyl-2-oxo-2,3-dihydro-1*H*-pyrimidin-4-ylidene)-acetamidine (Chart 2).

The location of the NH proton in **5a** remains unresolved. Its resonance, observed at room temperature as broad singlet at $\delta 6.29$ in $\text{DMSO-}d_6$, is shifted at $\delta 5.50$ and 5.53 ppm in CD_3CN and CD_2Cl_2 , respectively, and attempts to observe a fine structure by lowering the temperature were unsuccessful. Moreover, whereas ^{31}P NMR spectra of **5b** are characterized by a sharp AB multiplet, those of the PMePh_2 analogue show that one part of the expected AB multiplet (at $\delta -8.0$, $^1J_{\text{PPt}} = 3300 \text{ Hz}$) is broad, in contrast with the sharp resonance at $\delta -6.5$ ($^1J_{\text{PPt}} = 3300 \text{ Hz}$) as depicted in Figure 6 (trace a), in which the spectrum of a fresh solution of **5a** in CD_2Cl_2 is reported.

As the temperature decreases, the spectrum becomes more complex, a series of changes leading to the appearance of two sets of resonances at -40°C (Figure 6, trace b). Similar temperature dependence and spectral patterns were observed in CD_3CN . In addition, in the $\{^1\text{H}\}^{13}\text{C}$ spectrum of **5a** the

(21) Montagner, D.; Longato, B. Unpublished results.

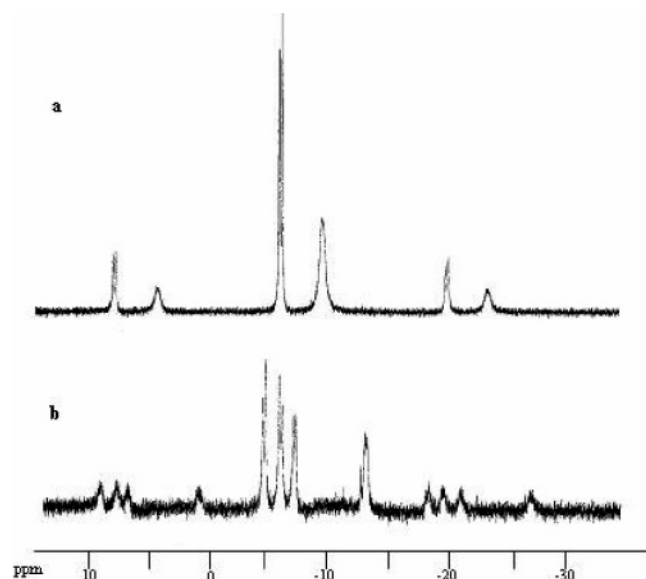


Figure 6. $^{31}\text{P}\{^1\text{H}\}$ NMR spectra of **5a** in CD_2Cl_2 : (a) fresh solution at 27 °C; (b) at -40 °C.

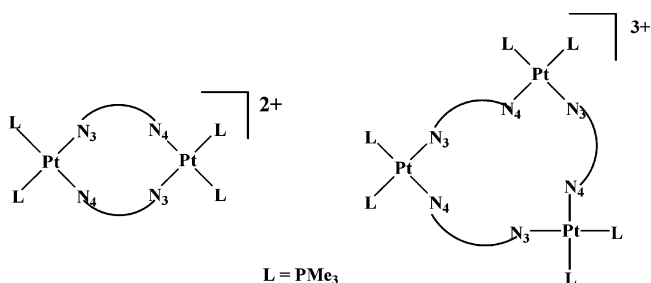
resonances of one phosphine appear broad (phenyl region) or undetectable (methyl region), while in the proton spectrum the two phosphines exhibit distinct signals for methyl groups, one sharp (at δ 1.87 with $^2J_{\text{HP}} = 10.5$ Hz and $^3J_{\text{HPt}} = 36$ Hz) and the other one broad (at 1.93 ppm $^2J_{\text{HP}}$ ca. 10 Hz with unresolved ^{195}Pt satellites).

These spectral features, not observed in the spectra of **3a**, are consistent with the presence of different conformations, related to restricted rotation of one phosphine around the Pt–P bond in complex **5a** and/or a different flexibility of the metallacycle. It is to be noted that in **3a** the $\{^1\text{H}\}^{13}\text{C}$ spectrum of the phenyl groups on the same phosphorus exhibits chemical equivalence (see experimental). This requires free rotation of phosphine ligands around the Pt–P bonds and/or the presence of a symmetry plane which can be obtained if the six atom metallacycle and the adjacent purine ring are coplanar. From a detailed analysis of the crystal structures of the two complexes it is apparent that there is a stacking interaction between the cytosine and the C(10) phenyl ring in **5a** (see Figure 5): the distance between their centroids is 3.86 Å, with torsion angle N(3)–Pt–P(1)–C(10) of -18.3° . The corresponding values in **3a** are 4.20 Å and 32.0° (N(1)–Pt–P(1)–C(1b)), respectively, with a tilting of the phenyl which does not provide a suitable stacking. It seems likely that the more bulkier carboxyl oxygen O(2) and methyl C(1) in the cytosine of **5a** might hamper or reduce the free rotation in solution of the adjacent phosphine group, when compared with that of the C(2)H environment in **3a**.

As shown for **3a,b**, complexes **5a** and **5b** in solution are stable only in acetonitrile. **5a** dissolved in a mixture of $\text{CD}_3\text{CN}/\text{CH}_3^{13}\text{CN}$ slowly (several hours at room temperature) exchanges the inserted acetonitrile molecule, indicating a kinetic lability of the chelated ligand.²² Moreover, **5a** and **5b** in chlorinated solvents lose acetonitrile to give species not yet completely characterized.

Role of the Phosphine Ligands in the Activation of CH_3CN . Previous studies showed that $\text{cis}[(\text{PMe}_3)_2\text{Pt}(\mu-$

Chart 3



$\text{OH})_2(\text{NO}_3)_2$, in water or DMSO, deprotonates the exocyclic NH_2 group of 1-MeCy affording the cyclic species $\text{cis}[(\text{PMe}_3)_2\text{Pt}\{1\text{-MeCy}(-\text{H})\}]_2(\text{NO}_3)_2$ with the cytosinate ion bridging two metal centers through the N(3) and N(4) atoms (Chart 3).²³ At 80 °C, it converts quantitatively in the corresponding trinuclear derivative, $\text{cis}[(\text{PMe}_3)_2\text{Pt}\{1\text{-MeCy}(-\text{H})\}]_3(\text{NO}_3)_3$, in which the nucleobase maintains the same coordination mode.²⁴

Some of the polynuclear cyclic complexes, previously characterized, have been now prepared in acetonitrile and their stability in this solvent verified. We find that the perchlorate salt $\text{cis}[(\text{PMe}_3)_2\text{Pt}\{9\text{-MeAd}(-\text{H})\}]_2(\text{ClO}_4)_2$ (soluble in CH_3CN , unlike its nitrate derivative),⁷ can be prepared in good yield from $\text{cis}[(\text{PMe}_3)_2\text{Pt}(\mu\text{-OH})_2(\text{ClO}_4)_2]$ and 9-MeAd in acetonitrile, and it is indefinitely stable in this solvent, even at 50 °C for a week. A similar stability is exhibited by the trinuclear species $\text{cis}[(\text{PMe}_2\text{Ph})_2\text{Pt}\{9\text{-MeAd}(-\text{H})\}]_3(\text{NO}_3)_3$ and $\text{cis}[(\text{PMe}_2\text{Ph})_2\text{Pt}\{1\text{-MeCy}(-\text{H})\}]_3(\text{NO}_3)_3$ which are quantitatively formed when $\text{cis}[(\text{PMe}_2\text{Ph})_2\text{Pt}(\mu\text{-OH})_2(\text{NO}_3)_2]$ reacts with 9-MeAd and 1-MeCy, respectively, in CD_3CN .^{10,13}

The formation of the insertion products **3a,b** and **5a,b** seems therefore related to the presence of the PMePh_2 and PPh_3 ligands in the starting hydroxo complex. However, the relative importance of steric and/or electronic factors of the phosphines on the metal coordination of CH_3CN and the following nucleophilic attack of the deprotonated nucleobase have to be elucidated. We observe that the trinuclear cation **2a** can be isolated from acetonitrile while the formation of its PPh_3 analogue is prevented, also in chlorinated solvents. As previously noticed, **2a** in $\text{DMSO}-d_6$ undergoes a complete and rapid rearrangement with formation of the mononuclear cation **4a** as the major component of the resulting mixture.⁵ On the contrary, in the same solvent, $\text{cis}[(\text{PMe}_2\text{Ph})_2\text{Pt}\{9\text{-MeAd}(-\text{H})\}]_3^{3+}$ maintains almost completely its trinuclear structure.⁸ Similarly, the cytosine complex $\text{cis}[(\text{PMe}_2\text{Ph})_2\text{Pt}\{1\text{-MeCy}(-\text{H})\}]_3^{3+}$ appears stable in DMSO, whereas we were unable to characterize similar species stabilized by PMePh_2 and PPh_3 .²¹

Conclusions

The formation of compounds **3** and **5** here described represents a rare example of a reaction in which a platinum–

- (22) Wagner, G.; Pakhomova, T. B.; Bokack, N. A.; Fraústo da Silva, J. J. R.; Vicente, J.; Pombeiro, A. J. L.; Kukushkin, V. Yu. *Inorg. Chem.* **2001**, *40*, 1683–1689.
- (23) Trovò, G.; Bandoli, G.; Casellato, U.; Corain, B.; Nicolini, M.; Longato, B. *Inorg. Chem.* **1990**, *29*, 4616–4621.
- (24) Schenetti, L.; Bandoli, G.; Dolmella, A.; Trovò, G.; Longato, B. *Inorg. Chem.* **1994**, *33*, 3169–3176.

nitrogen bond is *formally* added to a nitrile triple bond. The quality of the structural data obtained in the solid phase for these metallacycles does not allow us to discriminate between the azavinylidene complexes $cis\text{-}[L_2PtN=C(Me)\{\text{nucleobase}(-H)\}]^+$ and the imino structures $cis\text{-}[L_2PtNH=C(Me)\{\text{nucleobase}(-2H)\}]^+$, in which the hydrogen on the N(6) (or N(4)) atom of the NH_2 -deprotonated nucleobase is located on the nitrogen of the inserted CH_3CN molecule. This latter structure appears to be only detectable on the solutions of **3a,b** and **5b**. The existence of a possible tautomeric equilibrium between the two forms seems also ruled out on the basis of a detailed analysis of the NMR spectra obtained in various solvents. This possibility, however, cannot be excluded for complex **5a**.

All these metallacycles are stable only in acetonitrile solution. In chlorinated solvents, **3a** loses the inserted molecule of CH_3CN to give the trinuclear species **2a**, whereas **3b**, having the bulkier PPh_3 ligands, forms the mononuclear complex **4b**, stabilized by the chelation of the adenine at

the N(6), N(7) sites. For **2a** and **4b**, the insertion of CH_3CN into the platinum–nucleobase bond is a *reversible* reaction. On the contrary, for the cytosine derivatives **5a** and **5b**, the relatively low stability of the trinuclear species $cis\text{-}[L_2Pt\{1\text{-MeCy}(-H)\}]_3^{3+}$, when L is a $PMePh_2$ and PPh_3 , make the loss of acetonitrile an *irreversible* process.

Acknowledgment. This work was financially supported by the Ministero dell'Università e della Ricerca Scientifica e Tecnologica, PRIN 2004. Thanks are due to Consorzio Interuniversitario di Ricerca in Chimica dei Metalli nei Sistemi Biologici for a Grant to D.M. We are in debt with Professor L. Schenetti for the assistance on the $^{15}N, ^1H$ NMR experiments.

Supporting Information Available: Crystallographic data for the structures reported in this Article. This material is available free of charge via the Internet at <http://pubs.acs.org>.

IC051755F